Raman spectroscopy of stressed samples of oriented poly(ethylene terephthalate)

L. J. Fina*, D. I. Bower† and I. M. Ward
Department of Physics, The University of Leeds, Leeds LS2 9JT, UK
(Received 25 April 1988; accepted 8 July 1988)

Measurements of the shift and change of shape of the 1616 cm^{-1} Raman scattering peak of two moderately oriented samples of poly(ethylene terephthalate) (PET) under tensile loads of up to 0.2 GPa are reported, together with the corresponding strains. To obtain reproducible results load cycling procedures were adopted similar to those established for the study of viscoelastic behaviour. The Raman scattering was observed with polarized incident and scattered light, with the polarization directions either both parallel or both perpendicular to the draw direction in the samples. The results showed that for both samples the Raman shift was linearly related to the applied stress below the yield point. Up to the yield point very little change of line width was observed but above the yield point the width increased significantly. Differences in both widths and shifts were observed for the two polarization directions at the same stress level. The results are discussed in terms of the usual assumptions that the shift of the line gives a measure of the average stress in those chains which predominantly contribute to the peak and that the width and shape of the line give information about the spread of stresses. It is concluded that the technique can give useful information about the molecular stress distribution in thick samples of moderately oriented PET under load, including information about the different stress distributions on chains at different angles to the draw direction.

(Keywords: Raman spectroscopy; PET; orientation; stress distribution)

INTRODUCTION

The effects of applied stress on the positions and shapes of i.r. absorption and Raman scattering peaks have been studied by a number of authors. A substantial amount of work has been done on polypropylene[1,2], by i.r. spectroscopy, and more recently on diacetylenes[3] and on rigid rod polymers, such as PBT[4] and Kevlar[5], by Raman spectroscopy. A smaller amount of work has been done on polycarbonate[6], polystyrene[6], nylons[7,8], polyethylene[9,10] and poly(ethylene terephthalate) (PET)[7,8,11]. What is generally observed is a shifting and asymmetric broadening to lower wave numbers. This has been interpreted as being due to a stress induced change in the vibrational frequency for individual chains which do not all experience the same microscopic stress[9]. The observed line shape is usually assumed to be the convolution of the original line shape for the unstressed material with a function that describes the distribution of stresses, which can thus be studied[2]. Much of the previous work has been done on highly oriented systems, either in an attempt to understand the fundamental mechanisms of the effect or to use the effect as a microscopic strain gauge in the study of composites. We report here some measurements of Raman shifts in PET which show the potential of the method for the study of stress distributions in polymers of moderate degrees of orientation.

Earlier work on PET[7,8,11] has concentrated on the i.r. absorption at ~975 cm^{-1}, due to molecules with the *trans* conformation of the glycol residue, which has been shown to shift by about 20 cm^{-1} per GPa for 'highly oriented' samples[11]. We report here the results of a short study of the effects of stress on the Raman peak at 1616 cm^{-1} due to ring stretching. The study was designed to show whether Raman spectroscopy, which permits the use of thicker samples than can be used for i.r. spectroscopy, could provide useful information about molecular stresses in samples of moderate orientation. The 1616 cm^{-1} peak was chosen partly because it is well isolated and we have previously used it for studies of orientation[14,15], and partly because the effects of stress on the corresponding peak have been studied for some of the rigid rod polymers[4,5].

EXPERIMENTAL

Materials

Isotropic amorphous PET film was obtained from ICI Petrochemicals and Plastics Division, Wilton, England. The film had the following initial properties: density = 1.339 g cm^{-3}, refractive index = 1.577 and intrinsic viscosity = 0.68 dl g^{-1} Dumbbell-shaped samples of length 4 cm and width 7.5 cm in their central sections were cut and mounted in a tensile testing machine (RDP-Howden Ltd.) preheated to 80°C. The films were drawn at a rate of 5 mm min^{-1} to the desired draw ratio and allowed to cool to room temperature while held at the final strain. Following this drawing procedure, the samples were placed in an air oven at 60°C for five days to stabilize their properties. Refractive index measurements showed that the samples were uniaxially oriented to within the error of the measurements. The properties of the oriented films used in the present study are shown in *Table 1*. Tapes 1 mm wide by 3 cm long were cut from these films for examination by Raman spectroscopy and creep testing.

---

* Present address: The Department of Mechanics and Materials Science, Rutgers University, Piscataway, NJ 08854, USA
† To whom correspondence should be addressed

0032-3861/88/122146-06$03.00

Table 1 Properties of unloaded oriented PET films

Sample	Draw ratio	Thickness (μm)	Density (g cm^{-3})	Birefringence	$\langle P_2(\cos\theta)\rangle$†
1	3.6	93	1.353	0.085	0.37
2	4.6	56	1.363	0.130	0.57

† Calculated from the birefringence

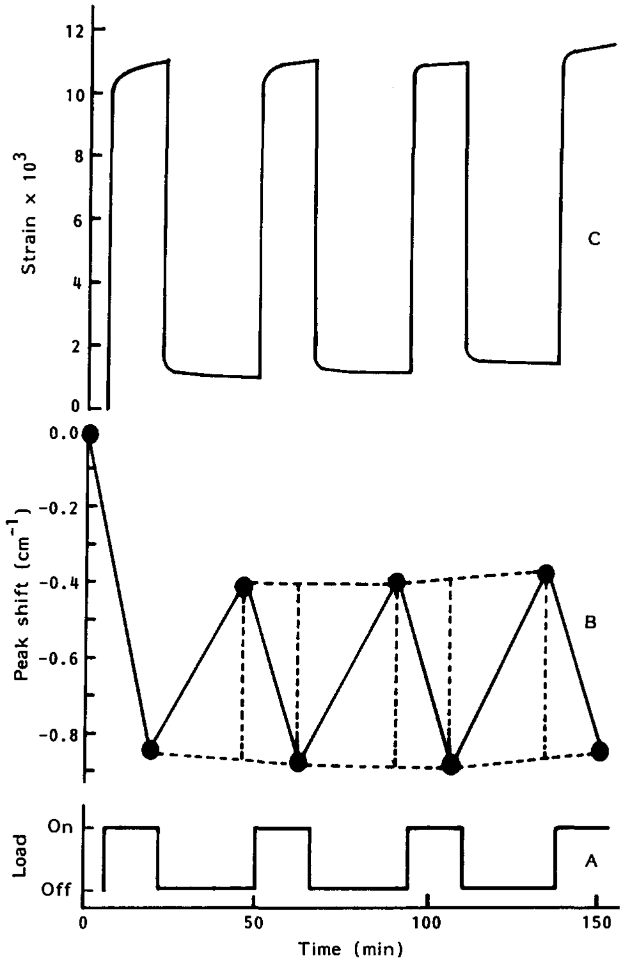

Figure 1 Position of Raman peak and value of strain as a function of time during load cycling. (A) Load cycle, (B) peak shift, (C) strain

Raman spectroscopy

Samples were illuminated by the beam from a Coherent Radiation Laboratories 52A Ar$^+$ laser tuned to 488 nm. The beam passed through a prism monochromator to remove plasma lines before reaching the sample. Light scattered from the sample, which was mounted with the normal to the film surface at about 50° to the incident beam, was collected in the 90° geometry by a focusing lens and passed through a quarter wave plate to eliminate preferential spectrometer response to polarized light. Most spectra were collected with the polarizer and analyser parallel to the draw direction, which was vertical, and these are called Vv spectra. A few spectra were collected with the polarizer and analyser horizontal and are called Hh spectra. The Raman scattered light was wavelength selected by a Coderg PHo double monochromator spectrometer, set to 4 cm^{-1} slit widths, and detected by a photomultiplier cooled to -30°C. The spectra were digitized by a Data Lab 4000 unit and transferred to a mainframe computer for processing.

The sample mount allowed dead loads to be applied to the sample. Preliminary experiments showed that the peak position of the 1616 cm^{-1} line remained constant after 10 s of loading to the maximum load to be used and after 3 min of unloading. Load cycling was therefore performed as shown in *Figure 1A* for each of a series of loads giving nominal stresses in the range 0–0.13 GPa for sample 1, which showed necking on loading above about 0.09 GPa, and nominal stresses in the range 0–0.18 GPa for sample 2, which did not show necking. Vv spectra were obtained by making four scans from 1600 to 1630 cm^{-1} during the last six minutes of a loaded or unloaded period and co-adding the intensities. These spectra allowed the shifts of the peaks on loading to be determined. A fresh piece was cut from the sample for each different load used in these load cycling experiments. A typical plot of peak shift obtained in such an experiment is shown in *Figure 1B*. The method of determining the peak shift is discussed below.

In order to study the line shapes more precisely, Vv and Hh spectra were obtained in the range 1537–1665 cm^{-1} for the drawn but unloaded material of sample 2 and for the drawn material of sample 2 under a nominal stress of 0.20 GPa. For these spectra, 40 or 50 scans were co-added and they were corrected for slight changes in laser power during scanning.

Creep measurements

Creep and recovery measurements were performed at room temperature using a standard tensile dead-load creep extensometer apparatus[16] with the transducer (Penny and Giles Model LVDT DS1303) mounted on a rod beneath the bottom grip. The voltage readings from the transducer were converted to relative displacement by a digital micrometer. The voltage–displacement plot was found to be linear in a range of 3 mm. The data were digitized and corrected for transducer calibration and apparatus displacement. The loading cycle was exactly the same as that used in the Raman experiment and a typical creep recovery curve is shown schematically in *Figure 1C*. This cycling of the load to obtain reproducible results for both the Raman and creep measurements is in line with established conditioning procedures for the study of viscoelastic behaviour and the determination of isochronal creep moduli[15].

DATA ANALYSIS

Raman shifts

The position of the 1616 cm^{-1} line was found for each spectrum by fitting a Lorentzian curve and linear baseline to it and taking the centre of this curve as the position. Although there were systematic deviations from the

Table 2 Stress sensitivity and modulus for 1616 cm^{-1} peak

Sample	Draw ratio	Moduls (GPa)	Stress sensitivity (cm^{-1} GPa^{-1})
1	3.6	6.6±0.5	6.5±0.3
2	4.6	9.5±0.5	5.3±0.5

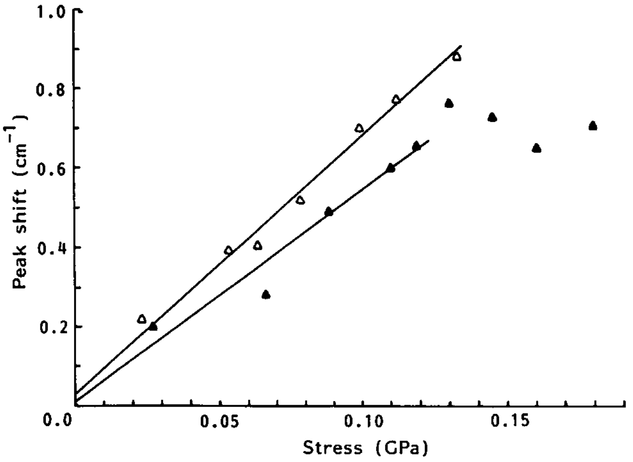

Figure 2 Raman peak shift S_c plotted against nominal stress. △, Sample 1; ▲, sample 2

Lorentzian line shape they were of the same general nature over the central part of the line. This suggests that the use of such fits in determining an average shift over the major part of the line shape is justified. It should be noted that the width of the required Lorentzian (full width at half intensity points) increased by about 10% from zero stress to the maximum stress used, i.e. from ~10 cm^{-1} to ~11 cm^{-1}.

The type of variation found for the positions in the load cycling experiment is shown in *Figure 1B*. For any load used in a cycling experiment we define two Raman peak shifts: the initial peak shift, S_i, observed on first loading the sample and the average cycling peak shift, S_c, calculated from four loaded and three unloaded spectra as the average of the five vertical differences indicated in *Figure 1B*. As expected, the scatter of the data for S_i was much greater than that for S_c because the sample is not well conditioned for the first loading, and the initial shifts will not, therefore, be discussed further. *Figure 2* shows S_c plotted against nominal stress for both samples. The lines shown are least squares fits to the initial linear regions and their gradients are given in *Table 2* as stress sensitivities.

The peak shifts found on loading to 0.20 GPa for the Vv and Hh spectra of sample 2 run over the longer wavenumber range were 1.22 and 0.40 cm^{-1}, respectively. These spectra were primarily intended for a detailed study of the change of line shape on loading. The positions of the peaks in the spectra of the unloaded sample differed by only 0.07 cm^{-1}.

Raman line shapes and widths

The fitting of Lorentzian curves to Vv spectra run in the range 1600–1630 cm^{-1} in order to obtain the peak positions also provided evidence about the changes in width of the central part of the peak. The widths of the peaks are plotted against stress in *Figure 3*.

For the Vv and Hh spectra of sample 2 run over the larger wavenumber range the changes in width on loading to 0.20 GPa, obtained from the fits, were 0.93 and 0.22 cm^{-1}, respectively. The width of the Vv spectrum of the unloaded sample (10.31 cm^{-1}) was greater by 0.41 cm^{-1} than that of the Hh spectrum.

Further information about changes in shape is provided by shifting the spectrum for a stressed sample relative to that of the unstressed sample along the frequency axis so that the maximum intensities of the peaks coincide, scaling the two spectra to the same maximum intensity and then subtracting the spectrum of the unstressed sample from that of the stressed sample. *Figure 4* shows examples of the result of this procedure applied to the Vv spectra for sample 2 for various stress levels. For each stress level all the loaded spectra were averaged and the result was smoothed using a cubic spline function. A similar procedure was applied to the unloaded spectra. A horizontal background equal to the value of the smoothed intensity at 1630 cm^{-1} was then subtracted from each

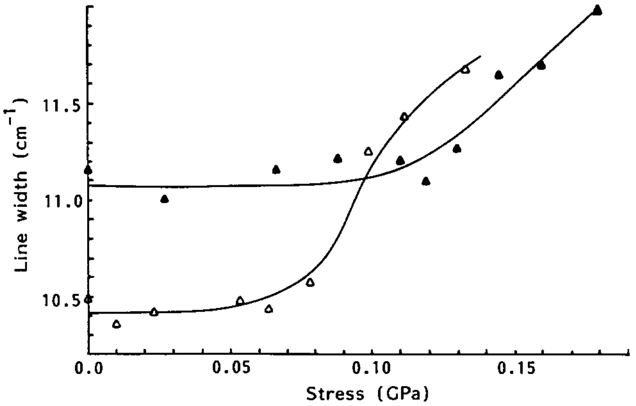

Figure 3 Raman peak width plotted against nominal stress. △, Sample 1; ▲, sample 2

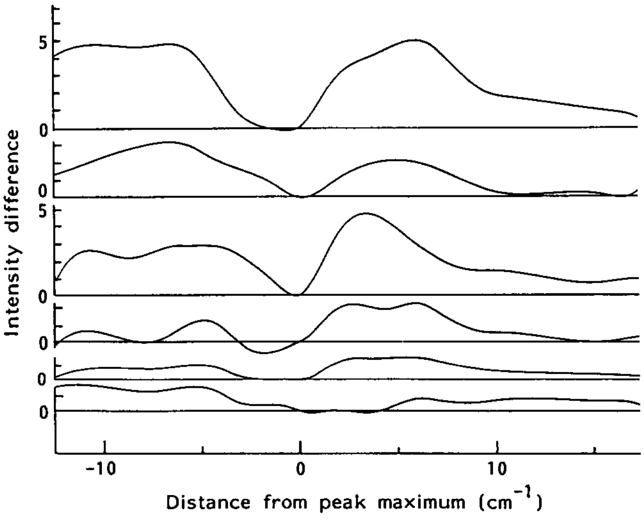

Figure 4 Differences between Raman line shapes for sample 2 loaded and unloaded (loaded–unloaded with peak for loaded sample shifted to coincide with that for the unloaded sample). The intensity difference is shown as a percentage of peak height. Nominal stresses (bottom to top) in GPa: 0.066, 0.088, 0.11, 0.13, 0.16, 0.18

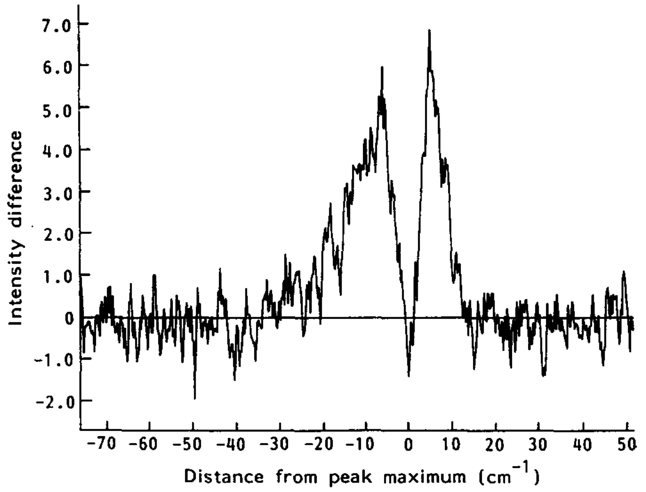

Figure 5 Difference between Raman line shapes (Vv spectrum) for sample 2 loaded to a nominal stress 0.20 GPa and unloaded (loaded–unloaded with peak for loaded sample shifted to coincide with that for the unloaded sample). The intensity difference is shown as a percentage of peak height

spectrum before the shifting, scaling and subtraction.

Similar subtractions were performed on the loaded (0.20 GPa) and unloaded spectra run on sample 2 in the extended range 1537–1665 cm^{-1}. Unfortunately, the Hh spectra were too noisy to give a convincing subtraction, even after smoothing, but the subtraction for the Vv spectra, to which no smoothing was applied, is shown in *Figure 5*. This figure shows that in addition to line broadening, indicated by the two peaks immediately on either side of the point corresponding to the original maxima before subtraction, the line shape for the loaded sample has a greater low wavenumber wing than that of the unloaded sample. This can also be seen in the original spectra shown in *Figure 6*.

We have attempted to deconvolute the spectrum of the loaded sample shown in *Figure 6* with the spectrum of the unloaded sample, but were unable to obtain a full deconvolution because of the noise level of the spectra. The results were, however, consistent with a narrow distribution of shifts peaked near the mean shift and having a width only about twice, or possibly less, than the shift, together with a wing of very much lower intensity on the low wavenumber side. The extent of this wing is best judged from the difference spectrum shown in *Figure 5*, which suggests that it extends for about 40 cm^{-1} from the peak.

Creep measurements

The creep data were analysed in a manner exactly analogous to the Raman shift data to provide initial strains, ε_i, and average isochronal strains, ε_c, for each stress level. Only the values of ε_c will be discussed. These are plotted against stress in *Figure 7*. The slopes of the best fit lines for the initial linear regions give the 16 min isochronal creep moduli. These are shown in *Table 2*.

DISCUSSION

Chain-orientation weighting of the Raman spectra

Before discussion of the detailed interpretation of the peak shifts and shape changes is undertaken, it is necessary to consider how the method of recording the Raman spectra weights the contributions of chains at different angles within the sample.

It has been shown[12] that the intensities of Raman scattering at 1616 cm^{-1} from uniaxially oriented PET are given, to a good approximation, by

$$I_{\mathrm{Vv}} = I_0(A - 2B\bar{P}_2^{\mathrm{r}} + 8C\bar{P}_4^{\mathrm{r}}) \qquad (1a)$$

$$I_{\mathrm{Hh}} = I_0(D + 2E\bar{P}_2^{\mathrm{r}} + C\bar{P}_4^{\mathrm{r}}) \qquad (1b)$$

where I_{Vv} and I_{Hh} are the intensities in the Vv and Hh spectra, I_0 is a constant, which depends on instrumental factors and on the absolute strength of the Raman scattering tensor, and the quantities A, B, C, D, and E depend on the ratios of the Raman tensor components for the line. The quantities $\bar{P}_2^{\mathrm{r}}$ and $\bar{P}_4^{\mathrm{r}}$ are the averages over the sample of the second and fourth order Legendre polynomials $P_2(\cos\theta_{\mathrm{r}})$ and $P_4(\cos\theta_{\mathrm{r}})$, where θ_{r} is the angle between the C_1–C_4 direction in a typical benzene ring and the draw direction. It has been shown[13] that the Raman tensor for the 1616 cm^{-1} ring mode has axes very close to those of the ring. It is very nearly cylindrically symmetric around C_1–C_4 with the ratio, r, of the component perpendicular to the C_1–C_4 direction to the component parallel to that direction having the value −0.18. The quantities A, B, C, D, and E have been given explicitly in terms of r in ref. 12.

If the C_1–C_4 direction makes the angle α with the local chain axis direction then, provided that there is no preferred orientation around the chain axes, the average value $\langle P_n(\cos\theta_{\mathrm{r}})\rangle$ of $P_n(\cos\theta_{\mathrm{r}})$ for those chains with axes at θ to the draw direction is given by

$$\langle P_n(\cos\theta_{\mathrm{r}})\rangle = P_n^{\theta} P_n^{\alpha} \qquad (2)$$

for $n=2$ and 4, with $P_n^{\theta} = P_n(\cos\theta)$ and $P_n^{\alpha} = P_n(\cos\alpha)$. If $N(\theta)\,\mathrm{d}\omega$ represents the fraction of chain axes lying within a small solid angle $\mathrm{d}\omega$ at any angle θ to the draw direction, it follows that the contributions to I_{Vv} and I_{Hh} of the chains lying within a range $\mathrm{d}\theta$ at θ to the draw direction are

$$I_{\mathrm{Vv}}(\theta)\,\mathrm{d}\theta = I_0(A - 2BP_2^{\theta}P_2^{\alpha} + 8CP_4^{\theta}P_4^{\alpha})N(\theta)\sin\theta\,\mathrm{d}\theta \qquad (3a)$$

$$I_{\mathrm{Hh}}(\theta)\,\mathrm{d}\theta = I_0(D + 2EP_2^{\theta}P_2^{\alpha} + CP_4^{\theta}P_4^{\alpha})N(\theta)\sin\theta\,\mathrm{d}\theta \qquad (3b)$$

If we assume that $N(\theta)$ is the most probable distribution

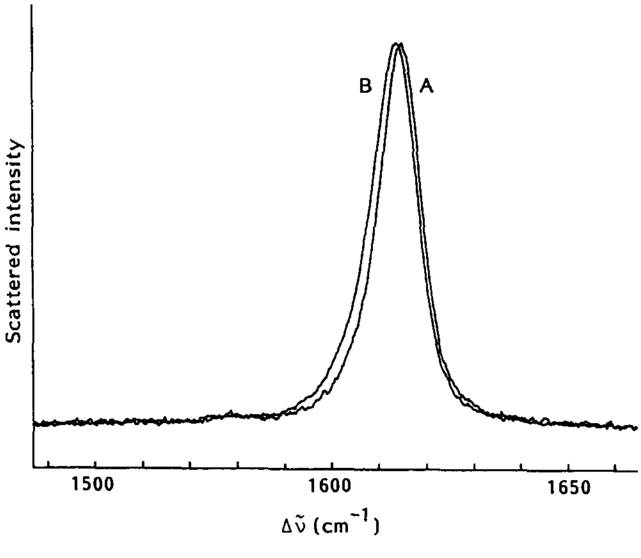

Figure 6 Vv spectra for sample 2 loaded to a nominal stress of 0.20 GPa and unloaded. (A) Unloaded; (B) loaded

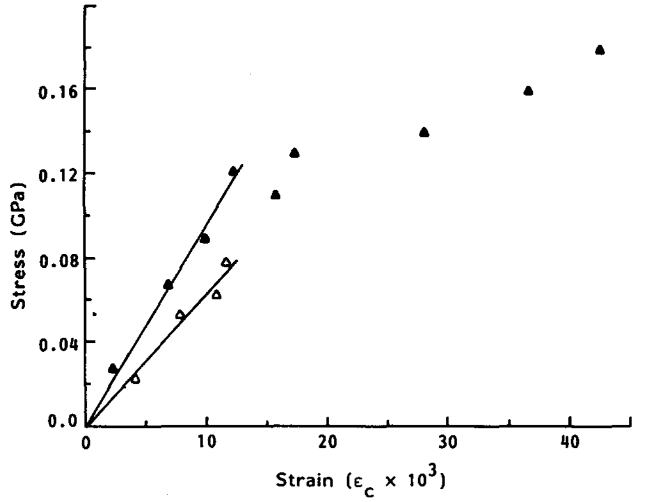

Figure 7 Strain ε_c plotted against nominal stress. △, Sample A; ▲, sample 2

for the value of $\langle P_2(\cos\theta)\rangle$ estimated from the birefringence of the sample, then[16]

$$N(\theta)=\exp[a_0+a_2P_2(\cos\theta)] \qquad (4)$$

with a_0 and a_2 chosen so that the integral of $N(\theta)$ over all solid angles is unity and the average value of $P_2(\cos\theta)$ for $N(\theta)$ is equal to the known value of $\langle P_2(\cos\theta)\rangle$.

Figure 8 shows the forms of $I_{\mathrm{Vv}}(\theta)$ and $I_{\mathrm{Hh}}(\theta)$ for sample 2 calculated from these equations. These plots show that I_{Vv} has the largest contribution from chains close to the draw direction, whereas I_{Hh} has the largest contribution from chains perpendicular to the draw direction.

Stress distribution

Sample 1 showed necking at nominal stresses above 0.09 GPa. This yielding is clearly shown in the width–stress data in *Figure 3*. For stresses lower than those which caused yielding very little line broadening was observed, although *Figure 2* shows that the peak shift remained linearly related to the stress right through the yield region. Evidence for the yielding of sample 2 at about 0.12–0.13 GPa is, however, visible on both the shift–stress and width–stress plots (*Figures 2* and *3*) as well as on the stress–strain curve (*Figure 7*) but no necking was observed for his sample. Again, the line width does not change significantly below the yield region but does change above, whereas the peak shift exhibits the opposite behaviour. We shall assume in the further discussion, as is usually done, that the shift of the line gives a measure of the average stress in those chains which predominantly contribute to the peak and that the width of the line gives a measure of the spread of stresses.

The fact that S_c for sample 1 appears to vary linearly with stress even when the stress goes above the yield stress may be accidental. Once the load has been first applied the sample has been cold drawn and is effectively a sample of higher orientation which no longer yields on application of the same load. The S_c *versus* stress relationship is not, however, very sensitive to orientation over a small range of orientations, as the difference between the gradients of the two lines in *Figure 2* shows. Any difference may not be seen over the small range of stresses available. In contrast, S_c for sample 2 appears to level off at the yield stress. This suggests that the majority of the chains that contribute to the Vv Raman scattering, i.e. those near the draw direction, do not support a higher load once the sample has begun to yield homogeneously. The increased applied stress must then be supported by a minority of overstressed chains. Only 5% of overstressed chains are required if they support an average load of order 20 times the load supported by a chain near the maximum in the stress distribution function. This is not unreasonable, because the total area of the peak to the left in *Figure 5* is about 6% of the area under the 1616 cm^{-1} peak and its mean shift is about 15 times the shift of the peak. The evidence from the Hh spectra for sample 2 suggests that the bulk of the chains oriented in directions well away from the draw direction have much lower average stresses than those oriented close to the draw direction.

Turning to the behaviour of the line widths (*Figure 3*) we see that the line widths for both samples show evidence above the yield point for a wider range of stresses among the majority of chains, as well as the increasing development of the low frequency tail, indicated in *Figure 4*. The Hh peak for sample 2 is narrower than the Vv peak, which suggests that the range of stresses experienced by the bulk of the chains oriented well away from the draw direction is also lower than that for the bulk of chains oriented close to the draw direction.

Comparison with earlier work

Mocherla and Statton[11] have examined the shift as a function of stress for the 976 cm^{-1} i.r. peak of three oriented PET samples with a range of moduli of about 4–10 GPa, which is very comparable to the moduli of our samples. They found that a minimum load, corresponding approximately to the end of the linear stress–strain relationship, had to be applied to each sample before any peak shift was observed, but we find no indication of this for the 1616 cm^{-1} Raman line. Above the threshold they found shifts of ~12 cm^{-1} GPa^{-1} for the sample of lowest modulus and ~20 cm^{-1} GPa^{-1} for that of highest modulus. Our values of ~6 cm^{-1} GPa^{-1}

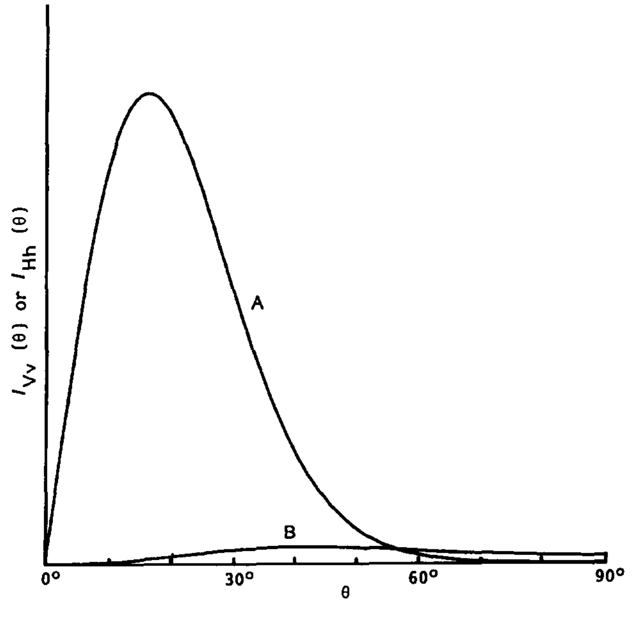

Figure 8 Chain-orientation weighting of Raman spectra for sample 2; (A) $I_{\mathrm{Vv}}(\theta)$, (B) $I_{\mathrm{Hh}}(\theta)$

for the 1616 cm^{-1} peak are somewhat smaller and, rather surprisingly, the value for the more oriented sample, sample 2, appears to be slightly lower than that for sample 1. Further work will, however, be required before we can be certain of this.

Day *et al.*[4] have made measurements of the shifts produced by applied stress for a number of peaks in the Raman spectra of samples of highly oriented poly(*p*-phenylene benzobisthiazole) (PBT), including that at 1600 cm^{-1}, which is believed to be due to a similar vibrational mode to that responsible for the 1616 cm^{-1} peak in PET. For this peak they found shifts equivalent to $\sim$3.2 cm^{-1} GPa^{-1}, although their data is presented in terms of strain sensitivity rather than stress sensitivity. Van der Zwaag *et al.*[5] have made similar measurements on the corresponding Raman peak at 1610 cm^{-1} for highly oriented samples of poly(*p*-phenylene terephthalamide) (PPTA) and found shifts equivalent to $\sim$3.3 cm^{-1} GPa^{-1}. In view of the differences in structure of the chains involved, of the degree of orientation of the samples and of the stresses used, which were an order of magnitude greater than ours, it is interesting to note the similarity in the stress sensitivities found for these materials to that found by us for PET.

CONCLUSIONS

Measurements of the shifts and changes of shape of the 1616 cm^{-1} Raman peak with applied stress can give useful information about the distribution of stresses on the molecules of thick samples of oriented PET under load and will therefore be a useful adjunct to studies of creep, yield and fracture. The method appears to be able to give information about the different stress distributions on chains at different angles to the draw direction.

REFERENCES

1 Wool, R. P. *J. Polym. Sci. Polym. Phys.* 1975, **13**, 1795
2 Wool, R. P. *Polym. Eng. Sci.* 1980, **20**, 805
3 Galiotis, C., Young, R. J., Yeung, P. H. and Batchelder, D. N. *J. Mater. Sci.* 1984, **19**, 3640
4 Day, R. J., Robinson, I. M., Zakikhani, M. and Young, R. J. *Polymer* 1987, **28**, 1833
5 van der Zwaag, S., Northolt, M. G., Young, R. J., Robinson, I. M., Galiotis, C. and Batchelder, D. N. *Polymer Comm.* 1987, **28**, 276
6 Evans, R. A. and Hallam, H. E. *Polymer* 1976, **17**, 838
7 Vettegren, V. I. and Novak, I. I. *J. Polym. Sci. Polym. Phys.* 1973, **11**, 2135
8 Zhurkov, S. N., Vettegren, V. I., Korsukov, V. E. and Novak, I. I. *Fracture 1969—Proc. 2nd Int. Conf. on Fracture, Brighton, UK*, (Ed. P. D. Pratt) Chapman and Hall, London, 1969, p. 545.
9 Bretzlaff, R. S. and Wool, R. P. *Macromolecules* 1983, **16**, 1907
10 Wool, R. P., Bretzlaff, R. S., Li, B. Y., Wang, C. H. and Boyd, R. H. *J. Polym. Sci. Polym. Phys.* 1986, **24**, 1039
11 Mocherla, K. K. R. *Ph.D. Thesis*, University of Utah, USA, 1976; Mocherla, K. K. R. and Statton, W. O. *J. Appl. Polym. Sci., Appl. Polym. Symp.* **31**, Fibre Science, 1977
12 Jarvis, D. A., Hutchinson, I. J., Bower, D. I. and Ward, I. M. *Polymer* 1980, **21**, 41
13 Purvis, J. and Bower, D. I. *J. Polym. Sci. Polym. Phys.* 1976, **14**, 1461
14 Gupta, V. B. and Ward, I. M. *J. Macromol. Sci. (Phys.)* 1967, **B1**, 373
15 Ward, I. M. 'Mechanical Properties of Solid Polymers', 2nd Edn, Wiley, Chichester, 1983, p. 109
16 Bower, D. I. *J. Polym. Sci. Polym. Phys.* 1981, **19**, 93